Novel Liquid Distributor Concept for Rotating Packed Beds

Pyka, T.; Bieberle, A.; Loll, R.; Held, C.; Schubert, M.; Schembecker, G.;

Originally published:

March 2023

Industrial & Engineering Chemistry Research 62(2023)14, 5984-5994

DOI: https://doi.org/10.1021/acs.iecr.3c00248

Liquid Distributor Design Study for Rotating Packed Beds

Tobias Pyka [a], *André Bieberle* [c], *Rouven Loll* [a], *Christoph Held* [a,d,*], *Markus Schubert* [c,e], *Gerhard Schembecker* [b]

[a] TU Dortmund University, Department of Biochemical and Chemical Engineering, Laboratory of Fluid Separations, Emil-Figge-Straße 70, 44227 Dortmund, Germany

[b] TU Dortmund University, Department of Biochemical and Chemical Engineering, Laboratory of Plant and Process Design, Emil-Figge-Straße 70, 44227 Dortmund, Germany

[c] Helmholtz-Zentrum Dresden-Rossendorf, Institute of Fluid Dynamics, Bautzner Landstraße 400, 01328 Dresden, Germany

[d] TU Dortmund University, Department of Biochemical and Chemical Engineering, Laboratory of Thermodynamics, Emil-Figge-Straße 70, 44227 Dortmund, Germany

[e] Dresden University of Technology, Chair of Chemical Process Engineering, Helmholtzstr. 14, 01069 Dresden, Germany

* Corresponding author. *Tel.*: +49 231 755 2086

E-mail address: christoph.held@tu-dortmund.de

Keywords: rotating packed bed, rotating baffle distributer, gamma-ray tomography

Abstract

Although it is known that a loss in separation performance is caused by liquid maldistribution, there is only marginal knowledge about liquid distribution in rotating packed beds (RPBs). As a result, the exact influence of liquid distribution on separation performance in RPBs is not fully understood. Therefore, this study focuses on the influence of different liquid distributors on the liquid distribution of a rotating metal foam packing inside RPBs. Liquid hold-ups were measured non-invasively using gamma-ray computed tomography (CT), and water/air was the system under investigation, operated at atmospheric pressure, temperature of 20°C, liquid flow rate of 60 l h^{-1}, F-factor of 2.3 $Pa^{0.5}$ and at rotational speeds up to 900 rpm. For the first time, the liquid distribution in axial direction of a rotating metal foam of an RPB could be accessed, which allowed the identification and quantification of occurring wall flows. Furthermore, the path of the liquid phase through the entire opaque packing could be visualized for different operating conditions by synchronizing the CT scans with the rotational speed of the rotor. The use of a single-point full-jet nozzle was more prone to cause wall flow than the use of a rotating baffle distributor with 36 baffles. For comparison, circumferential liquid maldistribution was also observed using a rotating baffle distributor with 12 baffles.

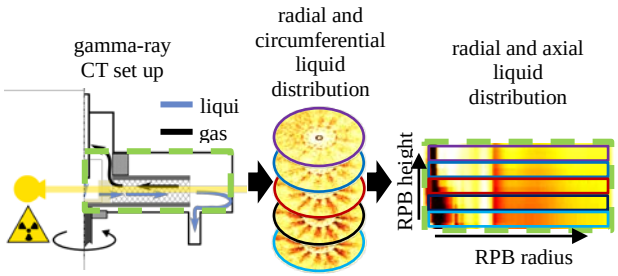

1. Introduction

In packed distillation columns, liquid maldistribution is the most significant reason for a loss of separation performance. Therefore, reducing the maldistribution is of particular interest [1]. Initial liquid distribution mainly influences the distribution behavior [2–4]. However, liquid maldistribution does not occur only in packed distillation columns but also in process intensification equipment such as rotating packed beds (RPBs). This is especially true for multi-rotor RPBs, since it is difficult to realize a well-defined liquid distribution [5, 6]. As depicted in Figure 1, the measurement of liquid maldistribution in an RPB, contrary to packed columns, cannot be performed via simple collecting devices below packing, as the packing rotates at high rotational speeds [2, 3, 5], and the liquid is gravitationally forced to flow over many axial rotor stages. For this reason, several methods have been developed to determine the liquid distribution in RPB packings.

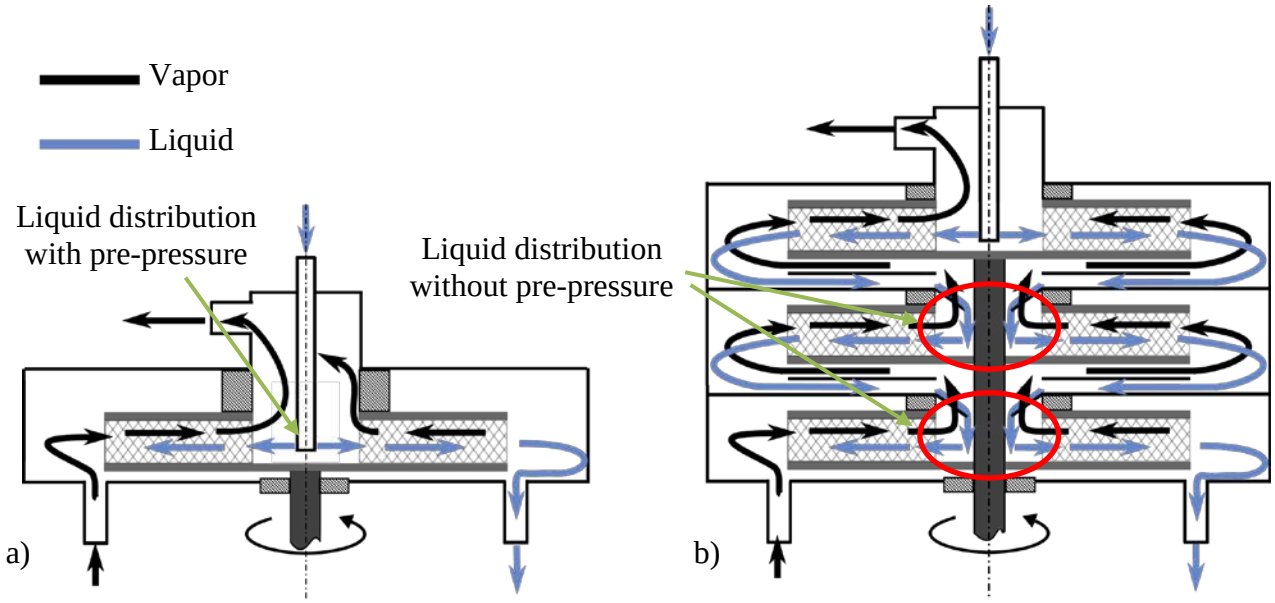

Figure 1. Comparison of a) single-rotor RPB with b) multi-rotor RPB principle with a special focus on liquid distribution.

The first attempt to study liquid distribution in RPBs was accomplished by Basic and Dudukovic [7] using conductance measurements inside the rotor. The rotor contained various-sized glass beads and it was operated with air, water, and four different propylene glycol solutions. Using this method, the obtained insights into liquid distribution in the radial and transverse directions revealed that the hydrodynamics of the RPB cannot be simplified as film flow [7]. Unfortunately, this type of measurement technique does not provide direct information on the flow pattern inside the packings [7]. Further studies determined the liquid distribution in the packings for single-rotor RPBs by visual observations [8–10], conductance probes [11], computed tomography (CT) [5, 12–15], and computational fluid dynamics [16, 17].

In 2019, Groß et al. [5] introduced gamma-ray CT for quantifying local liquid hold-ups in an RPB for the first time. By synchronizing the data acquisition of the CT scanner with the rotor speed (n_{rot}), cross-sectional gas-liquid phase distributions could be obtained with reference to sharply mapped rotating structures. Their study revealed the influence of different nozzle configurations and rotor internals on liquid maldistribution [5]. In 2021, Gładyszewski et al. [15] could verify an almost constant liquid hold-up along the radius using a carefully assembled anisotropic packing again using the gamma-ray CT. The results suggested that anisotropic packings could further enhance mass transfer [15]. Unfortunately, only 20 % of the packing height was scanned by Groß et al. [5] and Gładyszewski et al. [15], namely the axial center of the packing. Whether central radial and circumferential liquid distribution represents the entire packing height or not is still unknown.

Besides the packings, liquid distributors are another crucial part of RPBs that must also be considered for liquid distribution studies. This is especially true for multi-rotor RPBs applications, since conventional liquid distributors (e.g., a simple nozzle) cannot be implemented at lower rotor

stages due to the lack of a pressurized inlet (see Figure 1). A recent study by Pyka et al. [6] already revealed that the initial liquid distribution at lower rotor stages of multi-rotor RPBs must definitely be considered to prevent a severe loss of separation performance. Therefore, an easy-to-implement design of a liquid distributor for lower rotor stages was introduced, the so-called rotating baffle distributor (RBD), which resembles a rotary atomizer [6].

The current study aims at comparing the radial, the circumferential, and, for the first time, the axial liquid hold-up in an RPB using two different RBD designs and a conventional nozzle liquid distributor. This includes edge effects such as wall flow, which has not yet been analyzed in RPBs. Therefore, liquid maldistribution was studied in a water/air system in the RPB presented by Groß et al. [5] via rotation-synchronized gamma-ray CT measurement technique. Investigations were performed at various n_{rot} and fixed fluid flow rates. The results will also be used understand the separation performance improvements previously obtained by Pyka et al. [6] using an RBD with 36 baffles.

2. Material and Methods

2.1. Experimental setup

A sketch of the general experimental setup is presented in Figure 2, including an illustration of a radiographic scan acquired by moving the CT scanner in a fixed angular position over the height of the rotor section of the RPB.

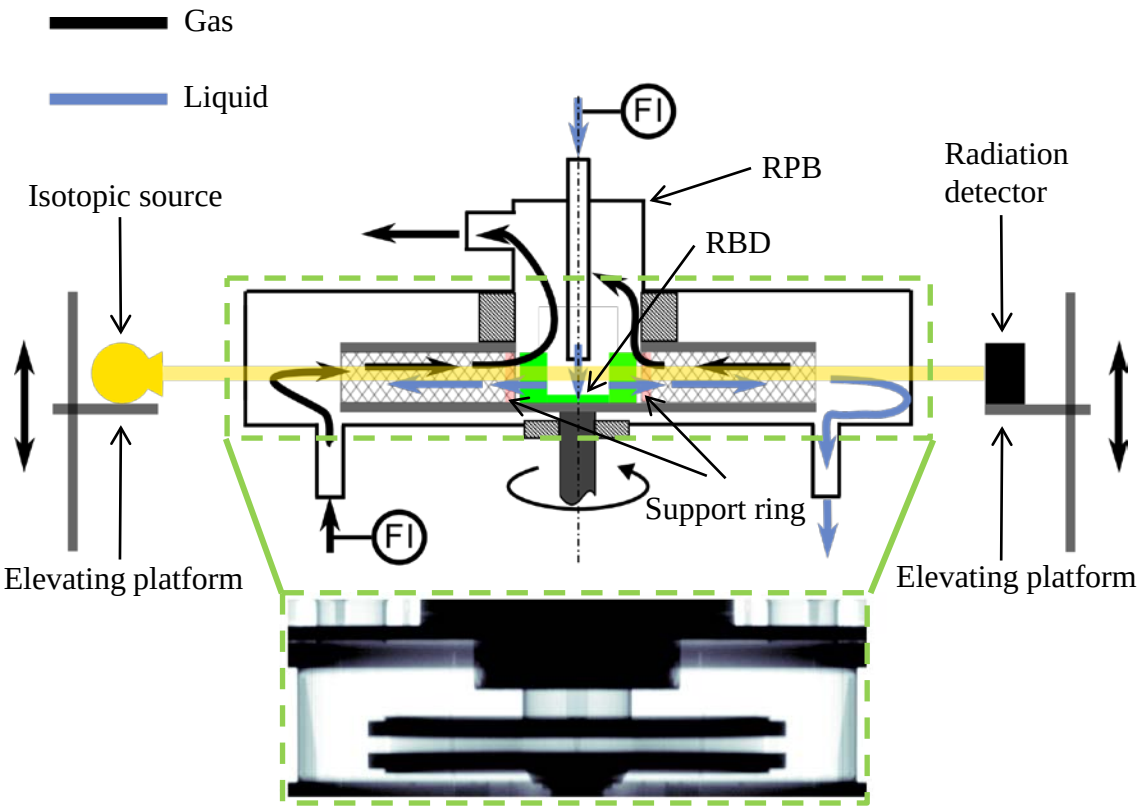

Figure 2. Sketch of the experimental setup (top) and radiographic scan (bottom). The RPB was operated in a counter-current mode. The cross-sectional liquid distribution as well as the averaged liquid hold-up in the metal foam packing was determined at different heights of the packing by moving the CT scanner along the axial direction of the RPB facility. Entering streams were measured via flow meters (FI).

The RPB was manufactured by ProCeler sp. z o.o (Warsaw, Poland) and is equipped with a metal foam packing from RECEMAT BV (Dodewaard, Netherlands). The installed support ring consists of twelve equidistant vertical struts, giving a free cross-sectional area of 90%, almost close to the average porosity of the applied packing of 92%. Further specifications of the RPB and the metal foam packing can be taken from Table 1.

Table 1. Specification of RPB and metal foam packing.

RPB / packing property	
Outer rotor diameter / mm	500
Inner rotor diameter / mm	145
Packing height / mm	10
Specific surface area of metal foam / $m^2\ m^{-3}$	1000
Porosity of metal foam /$m^3 m^{-3}$	0.92
Estimated average pore size / mm	1.4
Material of metal foam	Nickel-chromium alloy

The liquid flow rate ($\dot{V}_L$) and the gas flow rate ($\dot{V}_G$) were measured by an electromagnetic flow meter (FMG92-PVDF-BSP, OMEGA Engineering GmbH, Germany, accuracy $\pm$1% of full scale) and a thermal mass flow meter (KMT-114R10L1NQ4, Kobold Messring GmbH, Germany, accuracy ±1.5% of measured value ±0.5% of full scale), respectively. In the current study, the RPB was operated in a counter-current mode, and three different liquid distributors were investigated, i.e. an RBD with 12 baffles (RBD-12), an RBD with 36 baffles (RBD-36), and a conventional single-point full-jet (SPFJ) nozzle with an orifice diameter of 1 mm. Schematics of both RBDs are shown in Figure 3. A supporting structure additionally reinforces all baffles on the RBD. Their working principle is described in detail in [6]. Compared to SPFJ nozzle liquid distributors, RBDs were directly attached to the lower rotor plate and, thus, rotate at the same n_{rot} as the packing. Contrary to liquid injection with SPFJ nozzles, the liquid is specifically accelerated at each new rotor stage using RBDs, which guarantee defined boundary conditions at each new rotor stage in terms of liquid distribution (see Figure 4). The angle of the droplet break-up can be determined by

connecting the outer edge of the baffle with the entry of liquid towards the packing (see Figure 4 c)).

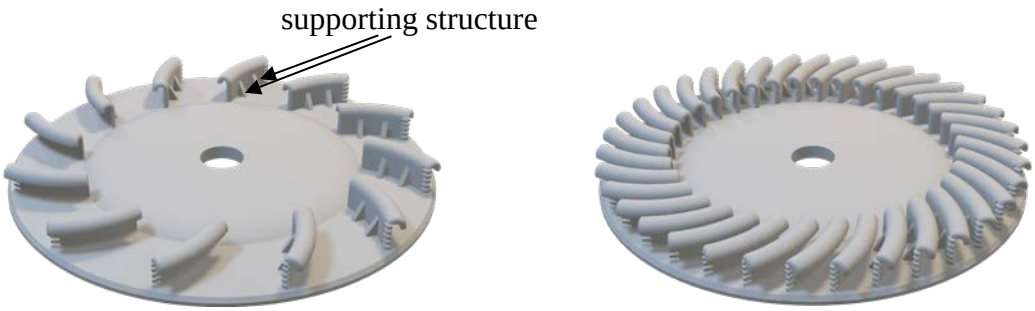

Figure 3. CAD drawings of the applied RBD in this study providing a) 12 baffles and b) 36 baffles.

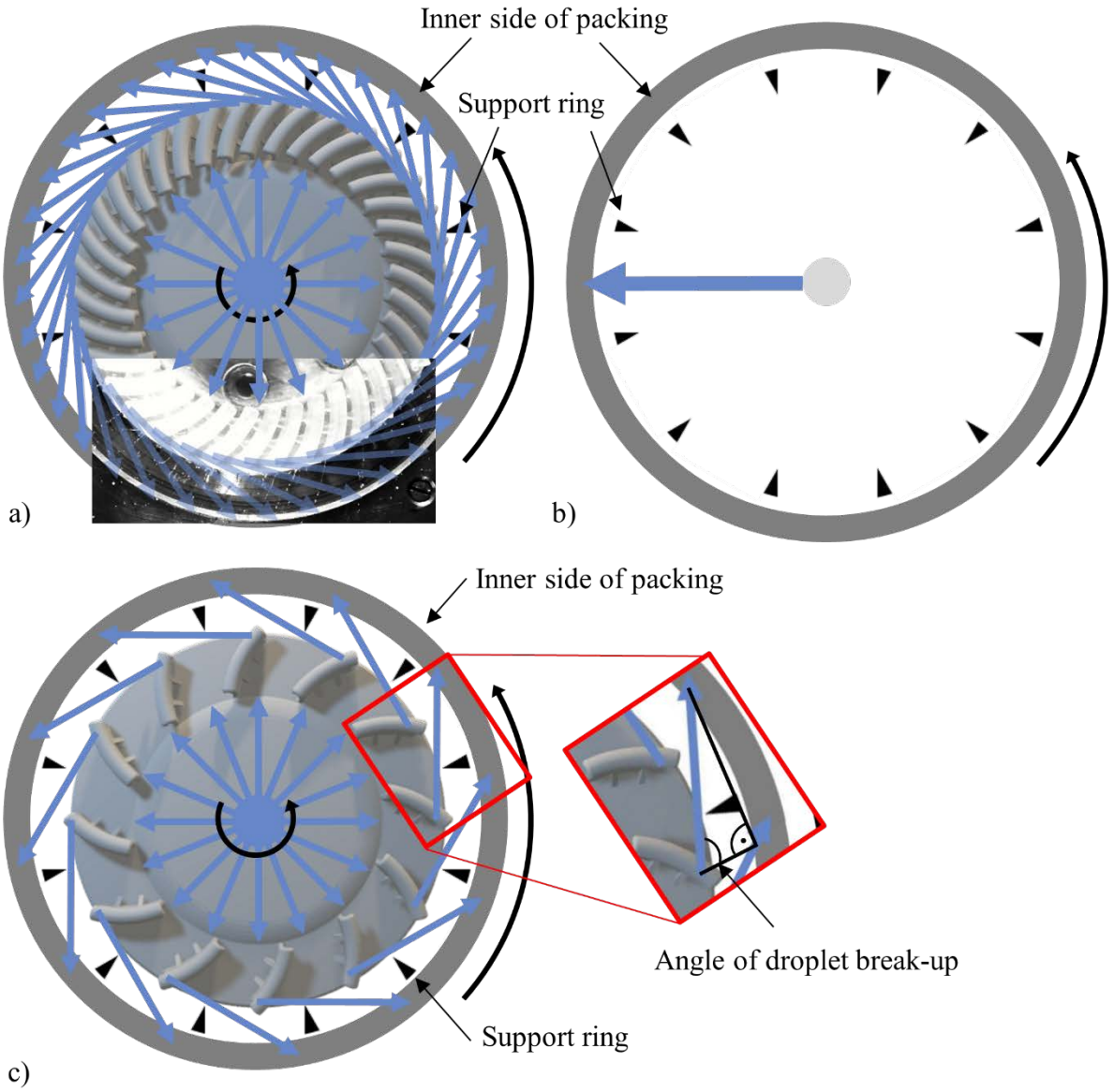

Figure 4. Top view and working principle of a) RBD-36, b) single-point full-jet (SPFJ) nozzle and c) RBD-12. Contrary to intuition, the liquid moves tangentially (proved by Pyka et al. [6]).

2.2 Experimental procedure

The current study used air and water as fluids at ambient temperature and pressure. In counter-current operation, $\dot{V}_{\mathrm{L}}$ and F-factor (F_{G}) were set to 60 l h^{-1} and 2.3 Pa$^{0.5}$, respectively, to realize identical operating conditions compared with the study of Pyka et al. [6]. n_{rot} of 300, 600 and 900 rpm were investigated since they showed the most severe influence on separation performance for the different liquid distributors used in the study of Pyka et al. [6].

The applied gamma-ray CT scanner was introduced by Hampel et al. [18] and Bieberle et al. [19], and specific details of its assembling to the pilot-scale RPB facility were described recently [5, 15]. However, to enable liquid hold-up measurements in different packing heights, the gamma-ray CT scanner is adjusted at different heights using a elevating platform (see Figure 2). Furthermore, the radiation fan beam is collimated to a height of 4 mm only. Five different axial measurement layers were selected in a step size of 1 mm to cover the entire metal foam packing height of 10 mm: 1) 1-5 mm, 2) 2-6 mm, 3) 3-7 mm, 4) 4-8 mm, and 5) 5-9 mm (see Figure 5).

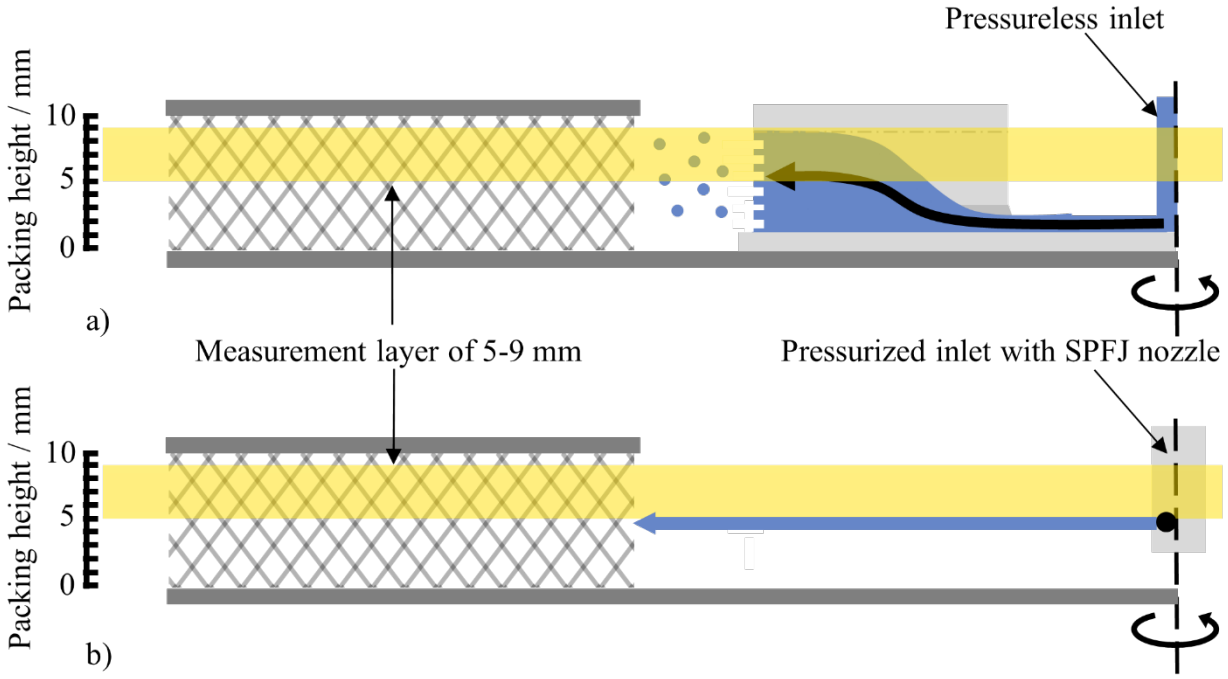

Figure 5. Side view illustrating the liquid injection into the metal foam packing using RBDs (a) and SPFJ (b). The upper CT scanning layer covers the packing height between 5 mm and 9 mm.

Before conducting gamma-ray CT scans, radiographic scans of the entire RPB were performed (see Figure 2) to ensure an almost plane-parallel orientation of the CT scanning layers compared with the metal foam packing. Data acquisition, synchronization with the RPB, and data processing including data reconstruction and liquid hold-up determination is described in detail by Loll et al. (2023).

3. Results and Discussion

3.1 Circumferential liquid distribution

As illustrated in Figure 3, both RBD designs consist of several identical radial-symmetric and angular-symmetric segments, namely 12 and 36 (3×12), respectively. Thus, the liquid distribution in each 30° segment can be assumed identical. Furthermore, the number of RBD segments is well-concerted with the number of support ring struts to provide an almost undisturbed liquid transfer

from the RBD into the packing. Thus, the liquid distribution in each 30° segment of the entire packing of the RPB can also be assumed identical. Finally, to enhance the liquid hold-up measurement accuracy and to ease comparisons of liquid hold-up measurements with those from SPFJ nozzle scans, segmentally-averaged circumferential liquid distributions of the analyzed packing layers are calculated. Additionally, the Polar-to-Cartesian transformed images are shown in Figure 6 for the three liquid distributors at constant n_{rot} = 300 rpm.

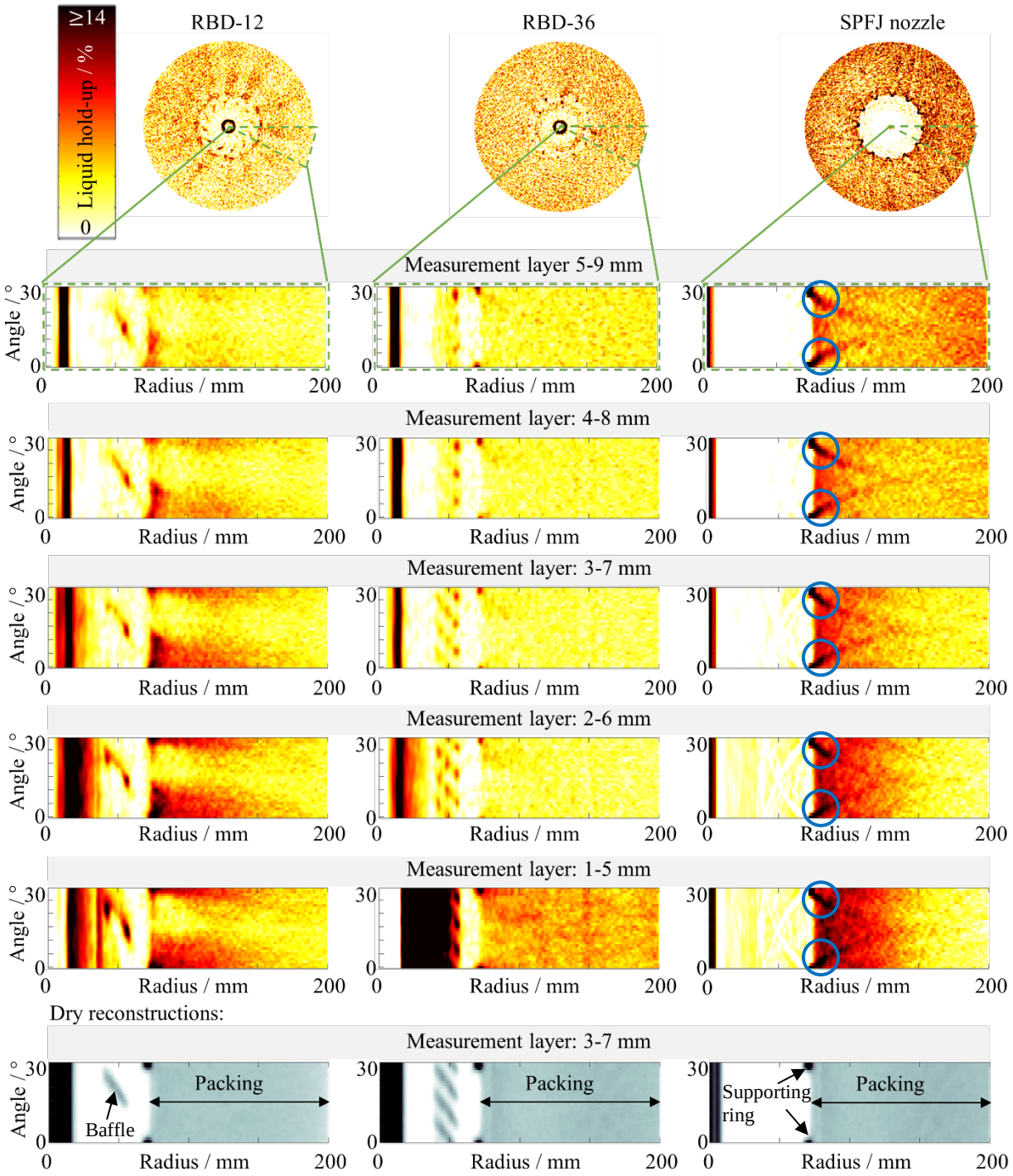

Figure 6. Segmentally-averaged circumferential liquid hold-ups for RBD-12, RBD-36, and SPFJ nozzle as liquid distributor at different packing layer heights and constant n_{rot} = 300 rpm, $\dot{V}_L$ = 60 l h^{-1}, F_G = 2.3 Pa$^{0.5}$, ambient pressure and temperature. Water/air were used as fluids. Blue circled: High liquid accumulation after supporting ring. Corresponding scans at dry condition are

presented at the bottom. The rotation direction is counterclockwise. For better visualization of the liquid hold-up in the packing, this is indicated from 0 to ≥14 %.

The packing starts at a radius of 81 mm (see Figure 6, dry reconstructions). Near the center of the RPB, liquid hold-ups ≥ 14 % represent the supplied liquid (see Figure 5), which is subsequently distributed via RBD or SPFJ nozzles. The liquid distribution within the packing is not uniform in the circumferential direction in all layers of the RPB operated with RBD-12, because the RBD-12 rotates with the same n_{rot} as the rotor, i.e. the packing. Thus, the liquid breaking up from the baffles is accelerated tangentially, leading to a liquid distribution into the packing (see Figure 4c). Therefore, the highest liquid hold-ups are present in the extension of a tangent in the circumferential direction from the baffles (see Figure 4c) and the lowest in between. Furthermore, it can be observed that although the liquid is introduced tangentially from the edge of the baffles to the packing inner side, it subsequently flows radially outwards to the outer packing side. In other words, the liquid flow inside the packing is mainly driven by the centrifugal field. This behavior was also noticed by Groß et al. [5]. Contrary to Yan et al. [9], no curved trajectory of liquid could be observed in the entry region of the packing. They explained the curvature by the relative movement in the circumferential direction of liquid entering the packing when using a nozzle as a liquid distributor [9]. Fortunately, this relative movement is minor when using RBDs.

Furthermore, while liquid accumulates at the support structures of the baffles, no significant liquid film can be detected at the baffles of the RBD-36 compared to the RBD-12. In the RBD-36, $\dot{V}_{\mathrm{L}}$ per baffle is three times lower compared to the RBD-12. In rotary atomizers, the break-up mechanism is not only dependent on n_{rot} but also on $\dot{V}_{\mathrm{L}}$ [20, 21]. Therefore, the combination of too-low $\dot{V}_{\mathrm{L}}$ (in this case: 60 l h^{-1}) and too-low n_{rot} (in this case: 300 rpm) do not lead to a film formation at the baffles, and eventually, no liquid breaks up at the baffles. Instead, the liquid simply

flows down to the lower rotor plate of the RPB. However, a high liquid accumulation is present at the baffles of RBD-12 and RBD-36 caused by the supporting structures (see Figure 3) and the liquid break-up at the outer edge of the baffle.

A uniform circumferential liquid distribution is achieved when using an SPFJ nozzle due to the high n_{rot}, although the liquid is statically introduced at one point only. This was also found by Groß et al. [5] and Pyka et al. [6]. Additionally, a high liquid accumulation is observed at the beginning of the packing of the initial and final angle of the sectionally averaged-circumferential liquid hold-up (see blue circles in Figure 6). This is attributed to the supporting ring (see Figure 4), which can be recognized in the dry reconstructions (see Figure 6). Here, the liquid is divided, which will be further discussed at n_{rot} = 900 rpm (see Figure 7).

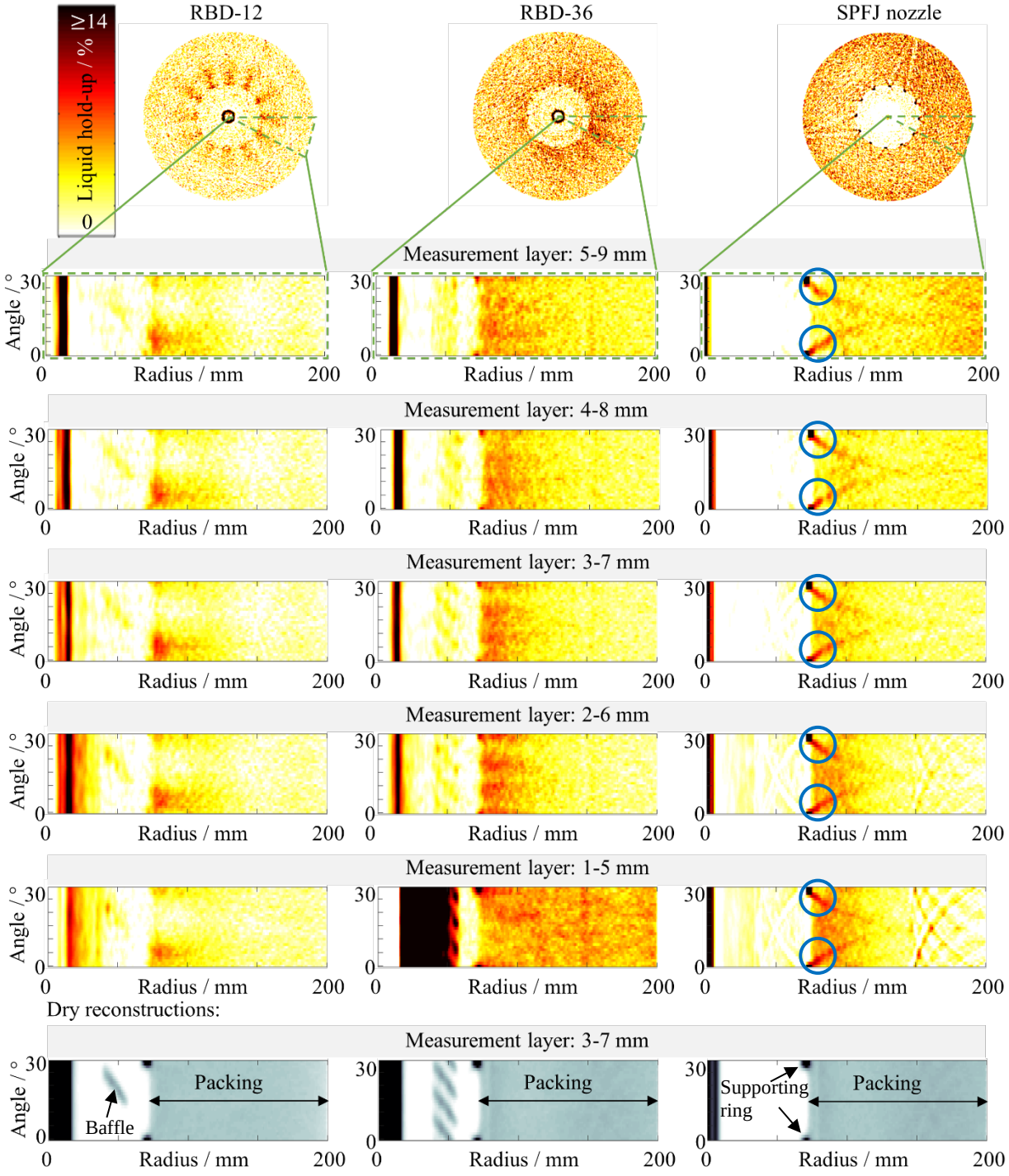

Figure 7. Segmentally-averaged circumferential liquid hold-ups for RBD-12, RBD-36, and SPFJ nozzle as liquid distributor at different packing layer heights and constant n_{rot} = 900 rpm, $\dot{V}_{\mathrm{L}}$ = 60 l h^{-1}, F_{G} = 2.3 Pa$^{0.5}$, ambient pressure and temperature. Water/air were used as fluids. Blue

circled: High liquid accumulation after supporting ring. Corresponding scans at dry condition are presented at the bottom. The rotation direction is counterclockwise. For better visualization of the liquid hold-up in the packing, this is indicated from 0 to ≥14 %.

Again, the liquid is suppled in the center (liquid hold-up ≥ 14 %) showing similar patterns, since it is independent of n_{rot} for the same measurement position. Generally, a lower liquid hold-up is obtained for the RBD-12 and the SPFJ nozzle at n_{rot} = 900 rpm compared to n_{rot} = 300 rpm due to the higher centrifugal acceleration. The liquid maldistribution within the packing generated by the RBD-12 is still visible at 900 rpm. The liquid hold-up decreases with increasing radius due to the increasing centrifugal acceleration.

A uniform circumferential liquid distribution in all measurement layers is achieved using the RBD-36 at n_{rot} = 900 rpm. In addition, film formation and liquid break-up at the baffles takes place at n_{rot} = 900 rpm contrary to n_{rot} = 300 rpm. Accordingly, higher liquid hold-up can be achieved with the RBD-36 at higher n_{rot}. This confirms that uniform circumferential liquid distribution can be achieved with RBDs when using enough baffles. The uniformity can be quantitatively expressed by the coefficient of variation (CV) of the liquid hold-up, which is the ratio of standard deviation and mean value. Therefore, a low CV implies a uniform liquid distribution. The CV of the liquid hold-up using different liquid distributors was determined for the first 10 mm inside the packing averaged over all measuring layers. This low packing depth was chosen to reduce the influence of increasing cross-sectional area with radius on the liquid hold-up generated by the different liquid distributors. The resulting CV values are summarized in Table 2.

Table 2. CV of the liquid hold-up for the first 10 mm of the packing using different liquid distributors at n_{rot} = 300 rpm and n_{rot} = 900 rpm.

	RBD-12	RBD-36	SPFJ nozzle
CV(n_{rot} = 300 rpm)	0.78	0.89	**0.40**
CV(n_{rot} = 900 rpm)	0.87	**0.46**	0.60

These CV results confirm the qualitative observations discussed above.

It should be noted that the circumferential distribution for the SPFJ nozzle is uniform regardless of n_{rot}. The same liquid accumulation at 900 rpm is similar to 300 rpm at the beginning of the packing of the initial and final angle (see blue circles in Figure 7). Remarkably, such liquid accumulation is not generated by the RBD-36, because packing with support ring are rotating, while the liquid jet of the nozzle is static, which shears the liquid. Less liquid shearing occurs using the RBD-36 since it rotates with the RPB and the relative slip is lower.

Figure 8 shows the average liquid hold-up based on the 12x30° sections and the five measurement layers of the first 10 mm inside the packing using the RBD-12 (detailed explanation in Appendix S1). Additionally, the full width at half maximum (FWHM) for each n_{rot} is drawn in Figure 8. FWHM is the width between two x-values whose y-values are on half maximum (detailed explanation of FWHM in Appendix S2). The x-values for the calculation of FWHM were interpolated.

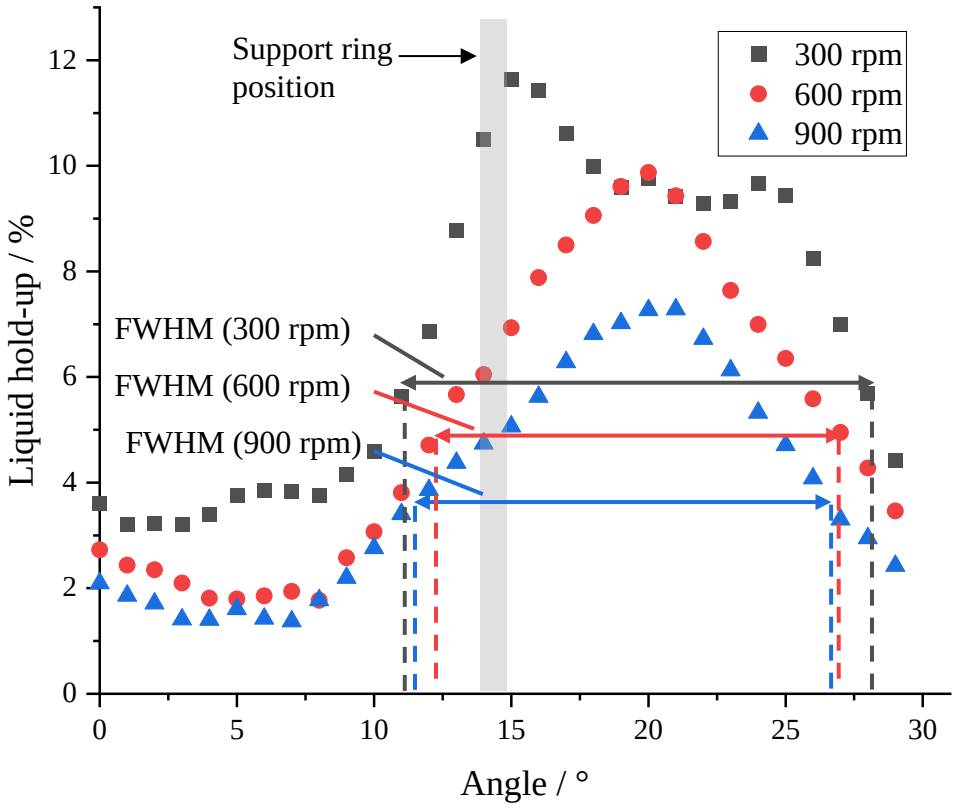

Figure 8. Liquid hold-up distributions in the segmental and packing height averaged 30° packing segment using the RBD-12, at n_{rot} = 300, 600, 900 rpm, $\dot{V}_L$ = 60 l h^{-1}, F_G = 2.3 Pa$^{0.5}$, ambient pressure and temperature. Water/air were used as fluids. FWHM of each n_{rot} is drawn.

For better visualization, the support ring position in Figure 8 is shown this time at 14° and 15°, while in Figure 6 and Figure 7, it was set at 0° and 30°; the relative position between the support ring and RBD-12 is unchanged (detailed explanation in Appendix S1). As previously shown in Figures 6 and 7, the liquid hold-up decreases with increasing n_{rot}. Also, the width of the distribution of the liquid hold-up initially decreases from FWHM(300 rpm) = 16.74 to FWHM(600 rpm) = 14.78 and then remains nearly constant at higher n_{rot}

(FWHM(900 rpm) = 15.04). That is because the width of the distribution of the droplets breaking up from the baffles becomes initially smaller due to the higher acceleration. The higher acceleration at higher n_{rot} also leads to a shift of the impact of the liquid on the packing towards larger angles. The liquid is more tangentially introduced to the packing (see Figure 4c) for $n_{\mathrm{rot}} \geq 600$ rpm compared with 300 rpm. At n_{rot} = 600 and n_{rot} = 900 rpm, the droplets break up at the baffle at an average angle of about 69° (angle drawn in Figure 4c) while an exclusive tangential break-up would result in an angle of 90°. Therefore, the droplets do not impinge the support ring (see Figure 4c). Due to the higher width of the distribution of the droplets breaking up from the baffles and the lower tangential trajectory of the droplets at 300 rpm, a part of the droplets impinge the support ring leading to a liquid accumulation. This liquid accumulation on the support ring could be prevented by shifting the relative position of the RBD-12 10° (clockwise) with respect to the support ring (see Figure 4 c).

Eventually, the angle of the droplets' trajectory could be calculated, showing that the droplets are not only accelerated tangentially when breaking up but also radially to some extent. These results demonstrate that using the RBD-36 can lead to a uniform circumferential liquid distribution, although a support ring occupies a marginal part of the cross-sectional area.

3.2 Axial liquid distribution

For improved visual and quantitative observations of the liquid distribution in the averaged axial section of the packing, the obtained angular-averaged radial liquid hold-up profiles from the CT scans are stacked together to a new axial liquid hold-up distribution that is, furthermore, up-scaled in packing height direction by the factor of two. Figure 9 compares the calculated axial

liquid distributions for the used liquid distributors and for n_{rot} = 300 rpm and n_{rot} = 900 rpm, respectively.

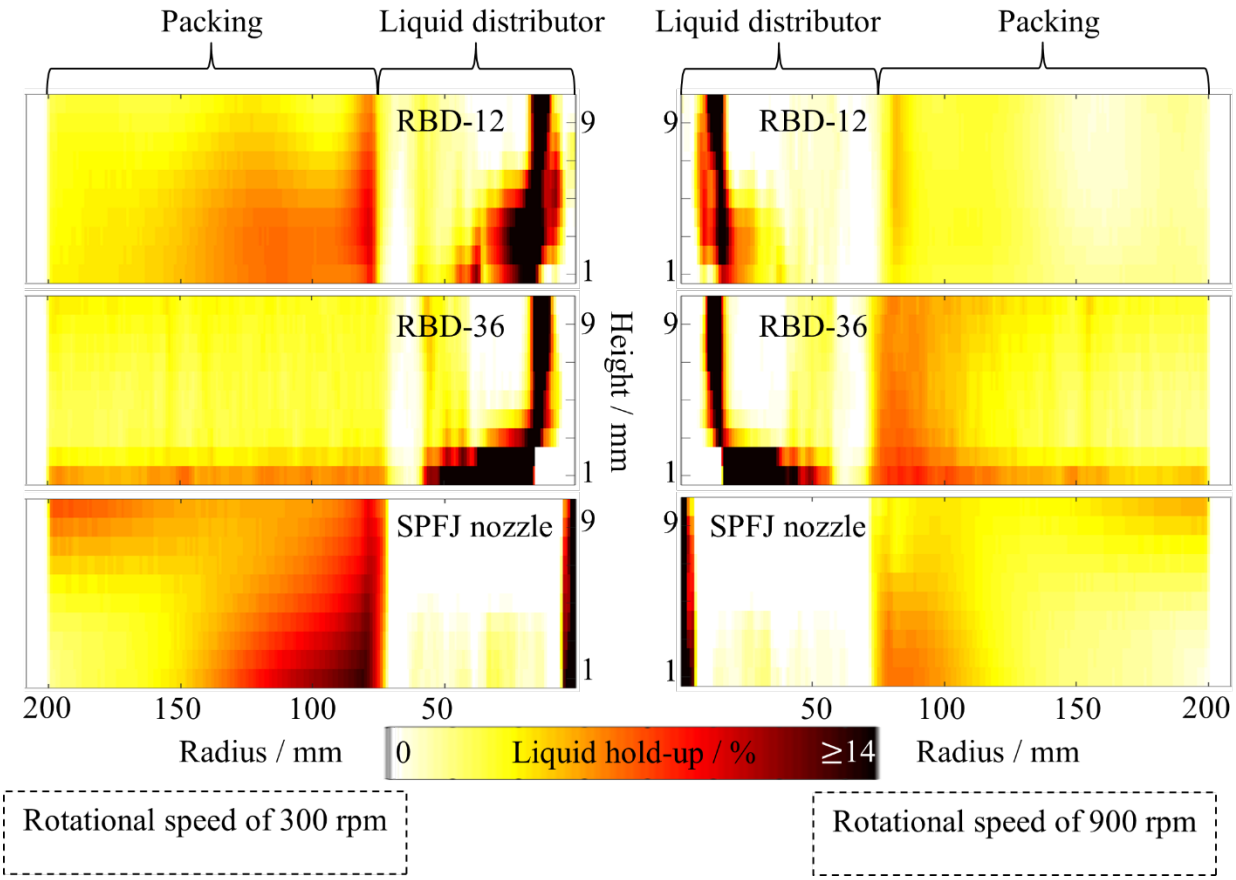

Figure 9. Comparison of axial liquid hold-up distributions using RBD-12, RBD-36, and SPFJ nozzle as liquid distributors for a packing height of 9 mm using different n_{rot} = 300 and n_{rot} = 900 rpm, $\dot{V}_L$ = 60 l h^{-1}, F_G = 2.3 Pa$^{0.5}$ as well as ambient pressure and temperature. Water/air were used as fluids.

Usually, the liquid hold-up decreases with increasing packing radius because the liquid is more accelerated with increasing radius. Figure 9 proves the capability of the RBD-12 to distribute the liquid axially at n_{rot} = 300 rpm. Surprisingly, using the RBD-36 does not provide such behavior.

Here, the liquid remains on the lower rotor plate. Therefore, the metal foam packing is not inherently capable of distributing the liquid axially. Remarkably, Pyka et al. [6] already identified a separation performance difference between RBD-12 and RBD-36 at 300 rpm. The new flow imaging results reveal that the higher separation performance with the RBD-12 is explicitly attributed to the better axial distributed liquid phase in the packing, i.e. a higher effective mass transfer area, compared to using the RBD-36.

At n_{rot} = 900 rpm, the axial liquid hold-up for the RBD-12 is the lowest compared to the other liquid distributors. That is because liquid maldistributions are present in the circumferential direction (see Figure 8). Nevertheless, a uniform liquid distribution in the axial direction could be achieved.

Using the RBD-36, the liquid in the entry region of the packing is also uniformly distributed. This observation confirms the capability of the RBD-36 to distribute the liquid uniformly in both the circumferential and axial directions. Taking a close look, a slightly increased liquid hold-up is obtained next to the inner packing inlet at the lower packing height. A possible explanation is that the liquid is partially breaking up at the plate of the RBD-36, as already observed in the visual study of Pyka et al. [6]. When the packing radius increases, the increased liquid break-up at the lower packing height increases the wall flow at the lower rotor plate. Therefore, the height of the plate of the RBD-36 should be decreased in the future to avoid a liquid break-up that favors wall flow.

Furthermore, the RBD-36 tend to induce a wall flow at the upper rotor plate. Similar to conventional distillation columns [1], such wall flow lead to separation performance losses since the effective mass transfer area is decreased. Although it is clearly notable that the liquid distribution is uniform in the first few millimeters of the packing, the liquid still accumulates at

the top and bottom rotor plates with increasing packing radius, resulting in dewetting in the center of the packing.

Analyzing the axial liquid distribution in the entry region of the packing using the SPFJ nozzle at 300 rpm suggests that the liquid jet did not impinge the packing exactly at its very axial center since a higher liquid hold-up is present in its lower half. The liquid moves with an increasing packing radius from the lower half to the upper half of the packing resulting in a wall flow (see Figure 10).

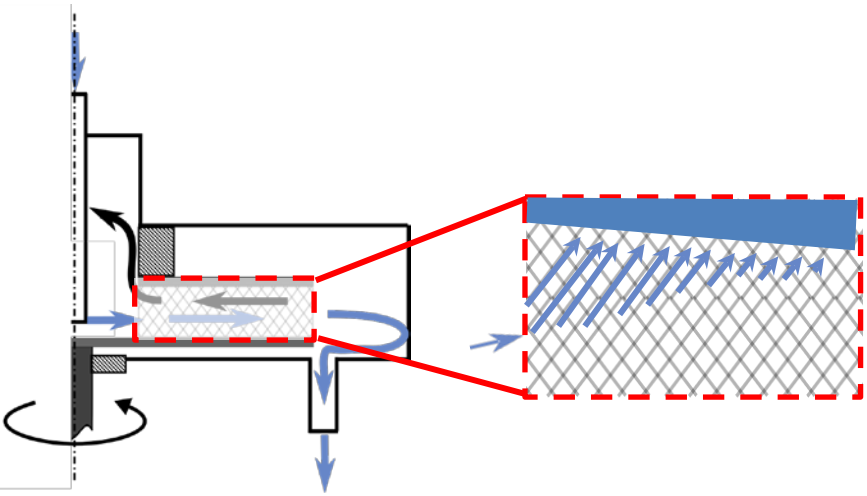

Figure 10. Schematic representation of the liquid distribution in axial direction generated by the SPFJ nozzle, which results in a wall flow at the upper rotor plate.

In 1996, Burns et al. [8] already speculated about a wall flow based on their visual observation, however, could not quantify it. The axial movement of the liquid can be explained by a not exactly perpendicular impingement of the liquid jet into the packing in the axial direction, which is, in fact, impossible for practical reasons. Instead, in our case, the liquid jet is slightly directed upwards (see Figure 10) and does not entirely lose the upward momentum upon impact with the highly porous packing (porosity of 0.92). The maintained momentum eventually leads to a movement of the liquid toward the upper rotor plate. Once the liquid reaches at the upper rotor plate, it remains there, analogous to the behavior of the liquid at the lower rotor plate using the RBD-36.

Consequently, it results in an accumulation of the liquid at the upper rotor plate with increasing radius.

The liquid movement towards the upper rotor plate with increasing packing radius is also present at n_{rot} = 900 rpm when using the SPFJ nozzle. A preferred direction of the metal foam can be rather excluded considering the results of the liquid hold-up obtained for the RBDs. The comparison of the two different of liquid distribution rather supports the hypothesis that the momentum of the liquid jet is maintained while impinging on the metal foam packing. The liquid does not have momentum in the axial direction when using RBDs as liquid distributors since it is solely accelerated into the tangential direction resulting in a wall flow at the upper and lower rotor plate with increasing radius. Another point supporting the hypothesis is the fact that the direction of deflection of the liquid jet by the support ring is maintained over tens of millimeters (see blue circles in Figures 6 and 7). By comparing the liquid hold-up using the RBD-36 with the SPFJ nozzle injection, it becomes apparent that the RBD-36 leads to higher liquid hold-up in the axial direction. When using the SPFJ nozzle, the packing is nearly completely dry at the outer radius and the lower packing half due to the movement of the liquid toward the upper rotor plate. This also explains the higher separation performance achieved when using the RBD-36 compared to the SPFJ nozzle at 900 rpm in the study of Pyka et al. [6]. Thus, using the RBD-36 leads to a more uniform liquid distribution of the packing, leading to better wetting and ultimately to a higher effective mass transfer area.

In summary, we measured the liquid hold-up in the axial direction of a metal foam packing inside an RPB over the entire packing height while using three different liquid distributors. The RBD-36 lead to a more uniform liquid distribution compared with RBD-12 and SPFJ nozzle at n_{rot} = 900 rpm, indicating that nozzles are more prone to inducing wall flow due to the pressurized

inlet. This wall flow will not be redistributed towards the packing but will accumulate with increasing packing radius. The results do not only explain the improved separation performance using the RBD-36 compared to the SPFJ nozzle, they also explain the limited scalability of single-block packings in terms of the radius [23, 24]. The increasing wall flow with increasing packing radius will lead to a decreasing effective mass transfer area with increasing packing radius. Therefore, internals are required to counteract the wall flow using single-block packings. Another way to counteract wall flow is to use packing structures that distribute the liquid inherently.

4. Conclusions

We presented a liquid hold-up study of three different liquid distributors applied in an RPB operated with water/air at atmospheric conditions for different rotational speeds. Determined liquid hold-up distributions using non-invasive gamma-ray CT can finally explain previously observed differences in separation performance depending on the installed type of liquid distributors. The tomographic data acquisition was synchronized with the rotating packing to investigate the liquid behavior within the rotating packing of 10 mm height. In addition, the angle of the break-up and the width of the distribution of the droplets from the baffles could be estimated.

The findings of this study enable future optimization of RBD designs with regard to the number of baffles and the plate to achieve high separation performance of multi-rotor RPBs. Furthermore, a systematic investigation of the influence of the entry angle of the liquid jet of a nozzle should be conducted to validate the hypothesis of maintaining the momentum of the liquid jet while entering the packing.

Author Contributions

The manuscript was written through the contributions of all authors. All authors have given approval to the final version of the manuscript.

Notes

The authors declare no competing financial interest.

Nomenclature

Latin letters

F_G	F-factor	$Pa^{0.5}$
n_{rot}	Rotational speed	rpm
$\dot{V}$	Flow rate	$L\ min^{-1}$

Subscripts

G	Gas
L	Liquid

Abbreviations

CT	Computed tomography
CV	Coefficient of variation
FI	Flow indicator
RBD-12	Rotating baffle distributor with 12 baffles
RBD-36	Rotating baffle distributor with 36 baffles
RPB	Rotating packed bed
SPFJ	Single-point full-jet

References

1. Spiegel L. The Maldistribution Story - An Industrial Perspective. Chemical Engineering Transactions; 2018(69): 715–20.
2. Olujić Ž, Jansen H. Large-diameter experimental evidence on liquid (mal)distribution properties of structured packings. Chemical Engineering Research and Design 2015; 99: 2–13.
3. Pavlenko A, Zhukov V, Pecherkin N et al. Investigation of flow parameters and efficiency of mixture separation on a structured packing. AIChE Journal 2014; 60(2): 690–705.
4. Veer KJRT, van der Klooster HW, Drinkenburg AAH. The influence of the initial liquid distribution on the efficiency of a packed column. Chemical Engineering Science 1980; 35(3): 759–61.
5. Groß K, Bieberle A, Gladyszewski K et al. Analysis of Flow Patterns in High-Gravity Equipment Using Gamma-Ray Computed Tomography. Chem. Ing. Tech. 2019; 91(7): 1032–40.
6. Pyka T, Brunert M, Koop J et al. Novel Liquid Distributor Concept for Rotating Packed Beds. Ind. Eng. Chem. Res. 2023; 62(14): 5984–94.
7. Bašić A, Duduković MP. Liquid hold-up in rotating packed beds: Examination of the film flow assumption. AIChE J 1995; 41(2): 301–16.
8. Burns JR, Ramshaw C. Process intensification: Visual study of liquid maldistribution in rotating packed beds. Chemical Engineering Science 1996; 51(8): 1347–52.
9. Yan Z-y, Lin C, Ruan Q. Hydrodynamics in a Rotating Packed Bed. I. A Novel Experimental Method. Ind. Eng. Chem. Res. 2012; 51(31): 10472–81.
10. Guo K, Guo F, Feng Y et al. Synchronous visual and RTD study on liquid flow in rotating packed-bed contactor. Chemical Engineering Science 2000; 55(9): 1699–706.
11. Burns JR, Jamil JN, Ramshaw C. Process intensification: operating characteristics of rotating packed beds — determination of liquid hold-up for a high-voidage structured packing. Chemical Engineering Science 2000; 55(13): 2401–15.
12. Yang Y, Xiang Y, Chu G et al. A noninvasive X-ray technique for determination of liquid hold-up in a rotating packed bed. Chemical Engineering Science 2015; 138: 244–55.
13. Liu Y-Z, Luo Y, Chu G-W et al. Liquid hold-up and wetting efficiency in a rotating trickle-bed reactor. AIChE J 2019; 65(8).
14. Liu W, Chu G-W, Luo Y et al. Mass transfer in a rotating packed bed reactor with a mesh-pin rotor: Modeling and experimental studies. Chemical Engineering Journal 2019; 369: 600–10.
15. Gładyszewski K, Groβ K, Bieberle A et al. Evaluation of performance improvements through application of anisotropic foam packings in rotating packed beds. Chemical Engineering Science 2021; 230: 116176.
16. Shi X, Xiang Y, Wen L-X, Chen J-F. CFD analysis of liquid phase flow in a rotating packed bed reactor. Chemical Engineering Journal 2013; 228: 1040–9.
17. Li Y-B, Wen Z-N, Sun B-C et al. Flow patterns, liquid hold-up, and wetting behavior of viscous liquids in a disk-distributor rotating packed bed. Chem. Eng. Sci. 2021; 252: 117256.
18. Hampel U, Bieberle A, Hoppe D et al. High resolution gamma-ray tomography scanner for flow measurement and non-destructive testing applications. Rev Sci Instrum 2007; 78(10): 103704.

19. Bieberle A, Schleicher E, Hampel U. Data acquisition system for angle synchronized γ-ray tomography of rapidly rotating objects. Meas. Sci. Technol. 2007; 18(11): 3384–90.
20. Wozniak G. Zerstäubungstechnik: Prinzipien, Verfahren, Geräte. Berlin: Springer: Berlin; 1. st ed; 1-186; 2003.
21. Rezayat S, Farshchi M, Ghorbanhoseini M. Primary breakup dynamics and spray characteristics of a rotary atomizer with radial-axial discharge channels. Int. J. Multiph. Flow 2019; 111: 315–38.
22. Pyka T, Koop J, Held C, Schembecker G. Dry Pressure Drop in a Two-Rotor Rotating Packed Bed. Ind. Eng. Chem. Res. 2022; 61(46): 17156–65.
23. Chen Y-S, Lin C-C, Liu H-S. Mass Transfer in a Rotating Packed Bed with Various Radii of the Bed. Ind. Eng. Chem. Res. 2005; 44(20): 7868–75.
24. Neumann K, Hunold S, Beer M de et al. Mass Transfer Studies in a Pilot Scale RPB with Different Packing Diameters. Ind. Eng. Chem. Res. 2018; 57(6): 2258–66.